CHAPTER 2

LITERATURE REVIEW

2.1 Introduction

This chapter highlights the information of carbon nanomaterials including their structure and properties as well as the techniques of producing them specifically in carbon vapor deposition method. Furthermore, their current applications and usefulness such as hydrogen storage are also included. In addition, the hydrogen adsorption measurements with several examples of previous study are discussed.

2.2 Nanoporous material

Nanoporous material is one of unique materials found in nanostructured materials (Lu et al., 2004). Because of its unique surface, structural and bulk properties, it can adsorb and interact with atoms, ions and molecules on their large interior surfaces and in the nanometer sized pore space. Being a subset of porous materials, the nanoporous material possesses a large porosities (more than 0.4) and pore diameters up to 100 nm (Holister et al., 2003).

Nanoporous materials could be natural or synthetic, organic or inorganic and hybrid in nature. The materials include carbon, silicon, alumino-silicates, polymers and metal oxides (Lu et al., 2004; Willems et al., 2005). This wide range of materials offers many applications such as in the area of environmental application, clean energy production and storage, catalysis and photocatalysis, sensors and actuators as well as biological applications.

For environmental application, a continuous invention and modification of adsorbent materials are required to remove SO_2, NO_x and VOCs emmisions efficiently (Gaur et al., 2006; Pietrzak et al., 2007). In addition, carbon nanotubes (CNTs) and carbon nanofibers also known as graphitic nanofibers (GNFs) provide good adsorbents for hydrogen storage in mobile application (Hong et al., 2006; Kim et al., 2005; Lachawiec et al., 2005; Sharon et al., 2007). The slit shaped pore size of CNTs and GNFs is the size of the inter planar spacing between the graphene planes. The spacing or the pore size is more than 0.335 nm (or some literatures quote as 0.34 nm) that is sufficient to accommodate H_2 molecules which has kinetic molecular diameter of 0.289 nm (Chambers et al., 1998).

Nanoporous materials also offer a desired microstructure and active site dispersion that are needed for improvement of catalytic activity and selectivity (Anandan, 2008; Doong et al., 2007). Due to their large surface area and high sensitivity to slight changes in environment (temperature, atmosphere, humidity and light), nanoporous materials are applicable in gas sensors (Cherevko et al., 2009; Umar et al., 2009). Because of material topography and spatial distribution of functional groups that control proteins, cells, and tissue interactions and bioseparations, applications in biotechnology is possible (He et al., 2009; Mostafavi et al., 2009).

In this chapter, the following section focuses on the application of clean energy production storage particularly on the capabilities of carbon nanomaterial acting as adsorbent to adsorb hydrogen gas.

2.3 Carbon nanomaterial

In general, carbon has two crystalline forms which are diamond and graphite. The former belongs to the face-centered cubic lattice. It possesses a characteristic of C-C single bonds between sp^3 hybridized carbon atoms in the cubic structure. Graphite is formed of stacked sheets with the carbon atoms in the basal plane arranged in *sp* tetragonal configuration. It has a two dimensional network which consists of regular

hexagons. The fourth electron is in a π orbital which is perpendicular to the weakly bonded hexagonal sheets. The distance between layers is much longer than the typical short carbon-carbon distance of hexagonal rings. Due to weak inter sheet bonding, graphite crystals are mainly affected by disorder along the c-axis whereas along the basal plane strong carbon-carbon bonding preserves a relatively high degree of order.

'Nano' is a prefix meaning one billionth (1/1,000,000) and this gives 'nanometer' as one billionth of a meter. Hence carbon nanotube (CNT) implies as a graphitic carbon form as a tube in a nanometer size. CNT was claimed to be found as early as 1889 as carbon filaments (Monthioux et al., 2006) but it was Sumio Iijima who had discovered multi-wall CNTs by capturing some images using transmission electron microscopy (TEM) in 1991. The CNTs which are developed from arc-discharge method were initially known as helical microtubules due to the structures that consists of long, thin cylinders of carbon (Iijima, 1991). CNT can be thought of as a sheet of graphite (a hexagonal lattice of carbon) rolled into a cylinder. This cylinder could be as a single or multiple cylindrical walls. The walls or graphene layers are parallel with the carbon filament axis. Both CNT and GNF can be found in a diameter range of 0.4 to 500 nm (Teo et al., 2003).

2.3.1 Bonding structure of carbon atom

An understanding of the bonding structure of carbon atoms is vital before knowing the structure of CNT. Carbon is the sixth elements in the periodic table and has the lowest atomic number of any elements in Group IV. A carbon atom has six electrons, which occupy $1s^2$, $2s^2$ and $2p^2$ atomic orbitals where the $1s^2$ orbital contains two strongly bound core electrons. Four more weakly electrons occupy $2s^2 2p^2$ valence orbitals (Endo et al., 2005). Since the energy difference between the upper $2p$ energy levels and the lower $2s$ level in carbon is small compared with the binding energy of chemical bond, the electronic wave functions for these four electrons can readily be mixed with each other.

The general mixing of 2*s* and 2*p* atomic orbitals are known as hybridization while the mixing of a single 2*s* electron with one, two or three 2*p* electrons is called sp^n hybridization where n=1,2,3, respectively. Therefore, three possible hybridizations occur in carbons that are *sp*, sp^2 and sp^3. The various bonding state results in certain structural arrangements where *sp* bonding gives rise to a chain structure such as carbynes, sp^2 bonding to planar structure such as graphene and sp^3 bonding to a tetrahedral structure such as diamond.

2.3.2 Bonding structure of CNTs

In graphite, three outer-shell electrons of each carbon atom occupy the sp^2 hybrid orbital to form three in-plane σ bonds with an out-of-plane π orbital (bond). This makes a planar hexagonal network. Van der Waals force holds sheets of hexagonal network parallel with each other with a spacing of 0.34 nm. Out-of-plane π orbital or electron is distributed over a graphite plane and makes it more thermally and electrically conductive. In addition, the interaction of the loose π electron with light causes the graphite to appear in black (Han, 2005).

CNT is a type of graphite where the graphene sheet rolled into a cylinder of nanometer size cylinder. Hence, bonding in CNTs is essentially sp^2. However, the circular curvature will cause quantum confinement and σ-π rehybridization in which three σ bonds are slightly out-of-plane. As a result, the π orbital is more delocalized outside the tube. This makes nanotubes mechanically stronger, electrically and thermally more conductive, and chemically and biologically more active than graphite (Han, 2005).

2.4 Types of carbon nanostructures

The discovery of carbon nanostructures begins in 1985 when Croto presented Buckminsterfullerene C_{60}. Later, more carbon nanostructures were found such as the family of fullerenes C_{70}, C_{76}, C_{84}, C_{60} in a crystalline form, carbon nanotubes, carbon nanocones, carbon nanohorns, nanoscale carbon toroidal structures and

many more (Osipov et al., 2005). In this section, the focus will be on carbon nanotubes (single and multi walled nanotubes) as well as carbon nanofibers (or also known as graphitic nanofibers).

2.4.1 Single wall nanotube

Single wall nanotube (SWNT) was first discovered in 1993 by Sumio Iijima (S. Iijima et al., 1993). SWNT is considered as a perfect graphene sheet in which the graphene being the same polyaromatic mono-atomic layer made of a hexagonal display of sp^2 hybridized carbon. The graphene sheet (see Figure 2.1) is rolled into a cylinder where the hexaganol rings are put in contact join coherently.

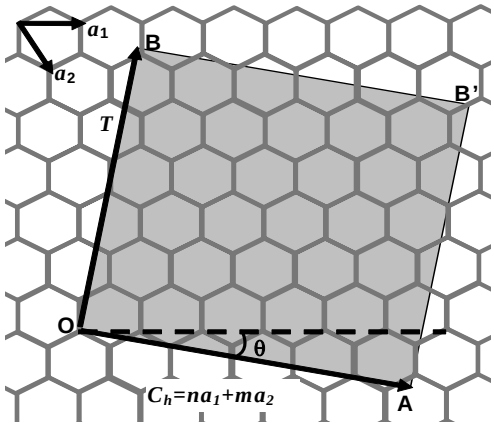

Figure 2.1 Structure of nanotube in a single graphite layer (Bhushan, 2004)

There are many ways to roll a grapheme into single-wall nanotube, some of the resulting nanotubes enabling symmetry mirrors both parallel and perpendicular to the nanotube axis like zigzag and armchair, respectively (refer Figure 2.2). Others are known as chiral or helical (Bhushan, 2004).

In Figure 2.1, a_1 and a_2 are defined as the unit vectors of the lattice with the C-C bond length being 1.42 Å. θ is a chiral angle between a_1 and C_h that will classify SWNTs. C_h is the chiral vector and T is referred as a translational vector which is perpendicular to C_h and points to the long axis of the SWNT (Cheng et al., 2004; D.

Lu, 2006). A SWNT is constructed by rolling the graphite layer along a certain direction $C_h=na_1+ma_2$ making OB and AB' coincide.

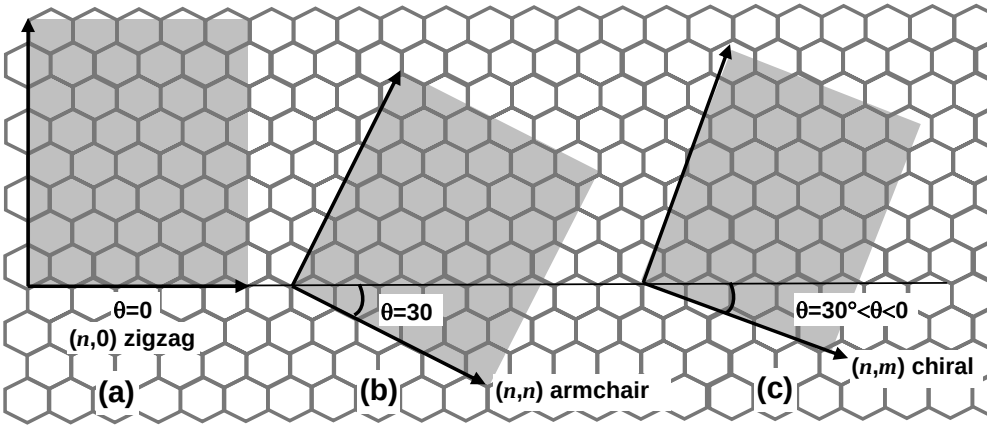

Figure 2.2 Three different ways of rolling a sheet of carbon atoms where depending on the direction the sheet is rolled into, three different patterns are emerged as (a) zigzag, (b) armchair and (c) chiral (Fischer, 2006).

By referring to Figure 2.2, depending on the chiral angle, a single-wall carbon nanotube can have three basic geometries. When m=0 the chiral angle is zero i.e. θ=0° the SWNT is defined as zigzag. If m=n, the chiral angle is 30° (θ=30°) the SWNT is defined as armchair whereas the SWNT is defined as chiral if 0<θ<30°.The various way to roll graphene tubes can be mathematically defined as follows:

$$OA \approx C_h = na_1 + ma_2 \tag{2.1}$$

$$\cos\theta = \frac{2n+m}{2\sqrt{n^2+m^2+nm}} \tag{2.2}$$

where $a_1 = \frac{a\sqrt{3}}{2}x + \frac{a}{2}y$, $a_2 = \frac{a\sqrt{3}}{2}x - \frac{a}{2}y$, $a = 2.46$ Å.

where n and m are the integers of the vector OA considering the unit vectors a_1 and a_2. The diameter D of the corresponding nanotube is related to C_h by the relation:

$$D = \frac{|C_h|}{\pi} = \frac{a_{c=c}\sqrt{3\left(n^2+m^2+nm\right)}}{\pi} \tag{2.3}$$

where 1.41 Å $\le a_{c=c} \le$ 1.44 Å
(graphite) (C_{60})

Obtaining values of *n* and *m* for a given SWNT is simple by counting the number of hexagons that separate the extremities of the C_h vector following the unit vector a_1 first then a_2 (Bhushan, 2004).Theoretical studies indicate that the physical and chemical properties of SWNTs are directly related to their structures. For example, when *n-m* or *2n+m=3k (k* is integer), the SWNT is metallic; in other cases, the SWNT is semi-conducting (Cheng et al., 2004).

2.4.2 Multiwall nanotube

Multiwall nanotube (MWNT) consists of SWNTs with regularly increasing diameters. The tubes are coaxially displayed according to a Russian-doll model (refer to Figure 2.3). The number of walls (or number of coaxial tube) can be anything starting from two, with no upper limit (Bhushan, 2004). The arrangement of the carbon atoms in the hexagonal network of the multi-wall carbon nanotube is often helicoidal, resulting in the formation of chiral tubes. Typical dimensions of multi-wall carbon nanotube are inner diameter: 1-3 nm, and length: 1-100 km (Cao, 2004).

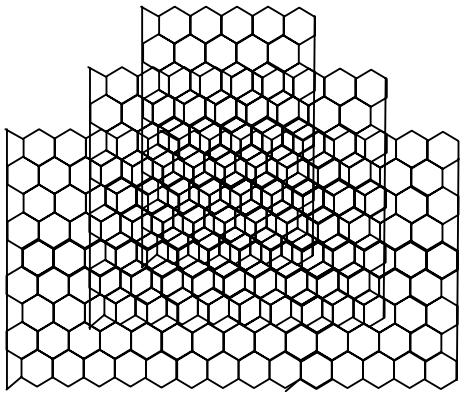

Figure 2.3 MWNT consists of several SWNTS with regularly increasing diameters (Ahwahnee Technology, 2004)

The intertube distance is approximately 0.34 nm and varies from 0.342 to 0.375 nm, depending on the diameter and number of nested shells of the MWNT. The increase in intershell spacing with decreased nanotube diameter is attributed to the increased repulsive force due to high curvature. (Goddard et al.,

2003). This interlayer spacing is approximately that of the intergraphene distance in turbostratic, polyaromatic solids (0.335 nm in genuine graphite), since the increasing radius of curvature imposed on the concentric graphenes prevents the carbon atoms from being displayed as in graphite i.e. each of the carbon atoms from a graphene facing alternatively either a ring center or a carbon atom from the neighboring graphene. The main structure in MWNT is known as concentric multiwall nanotube (c-MWNT). In this structure the concentric tubes of graphite oriented parallel to the carbon filament axis with a hollow core in the middle. Another texture known as herringbone structure (*h*-MWNT) or fishbone in which graphene make an angle with respect to the nanotube axis (Bhushan, 2004) (see Figure 2.4).

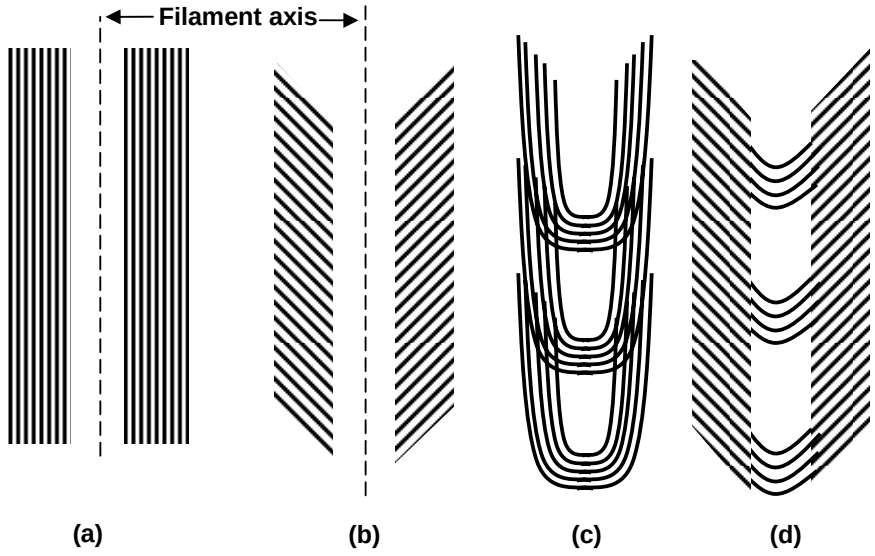

Figure 2.4 MWNT structure consists of (a) concentric MWNT; (b) herringbone MWNT or graphitic nanofibre (GNF); (c) bamboo-concentric MWNT; and (d) bamboo-herringbone MWNT (P. M. Ajayan, 1997; Bhushan, 2004)

The angle value varies upon the processing conditions (e.g. catalyst morphology or the atmosphere composition), from 0 (in this case the texture turn to *c*-MWNTs) to 90° (filament is no longer a tube). As for the latter, since the inner cavity is no longer opened all along the filament as it is for a genuine tube therefore they are referred as ‘nanofibres’ which is explained in the next topic. Another common feature is the occurrence, at a variable frequency, of a limited amount of graphenes oriented perpendicular to the nanotube axis, thus forming the so-called "bamboo"

texture. It cannot be a texture by its own but the effects are in a variable extent either *c*-MWNT (*bc*-MWNT) or *h*-MWNT (*bh*-MWNT) textures.

The structure of CNTs is basically a long, straight tube. It consists of pure hexagon arranged in a concentric manner. Apart from such structure, CNTs could also exist in a non-straight structure such as coiled, regular helical, rectangular, triangular, spring-like, double helical and branch-like structures. The formation of the bent or coiled structure is due to the incorporation of pentagon and hexagon pairs into hexagonal sheets, which then creates positively and negatively curved surfaces, whereas the formation of branched nanotubes occurs when a single tube splits into two smaller branches, or it could be additional nanotube growing out from another nanotube backbone (S. Huang et al., 2002.).

2.4.3 Graphitic nanofibers

One question has been raised whether nanofilaments like *h*-MWNTs can be addressed as nanotubes since the inner cavity is not opened all along the filament like any genuine tube. Besides having graphene planes at a certain angle to the filament axis, some graphene planes are perpendicular to the axis and stacked as piled-up plates. Hence, such as structures are referred as carbon nanofibers (CNFs) or graphitic nanofibers (GNFs) in literature (Bhushan, 2004). GNFs can be categorized into platelet (stacked) and herringbone or fishbone (cup-stacked) structures as in Figure 2.5.

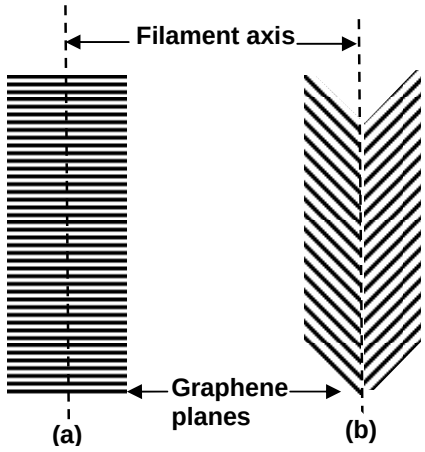

Figure 2.5 GNF structures that are (a) platelet and (b) herringbone structures.

The former structure is when the graphene layers perpendicular to the filament axis while the latter structure is when the graphene layers at a certain angle to the axis. The angle of conicity varies from 15° to 85° (Gogotsi et al., 2005).

2.5 Preparation of CNTs and GNFs

The main methods to develop CNTs can be classified into two categories, which are carbon vaporization and catalytic chemical vapor deposition (CVD) of hydrocarbon methods (Cheng et al., 2004). As described in (Daenen et al., 2003), the methods of synthesizing CNTs including the types of CVD methods are summarized in Figure 2.6. The brief description of each of them is explained in the following section.

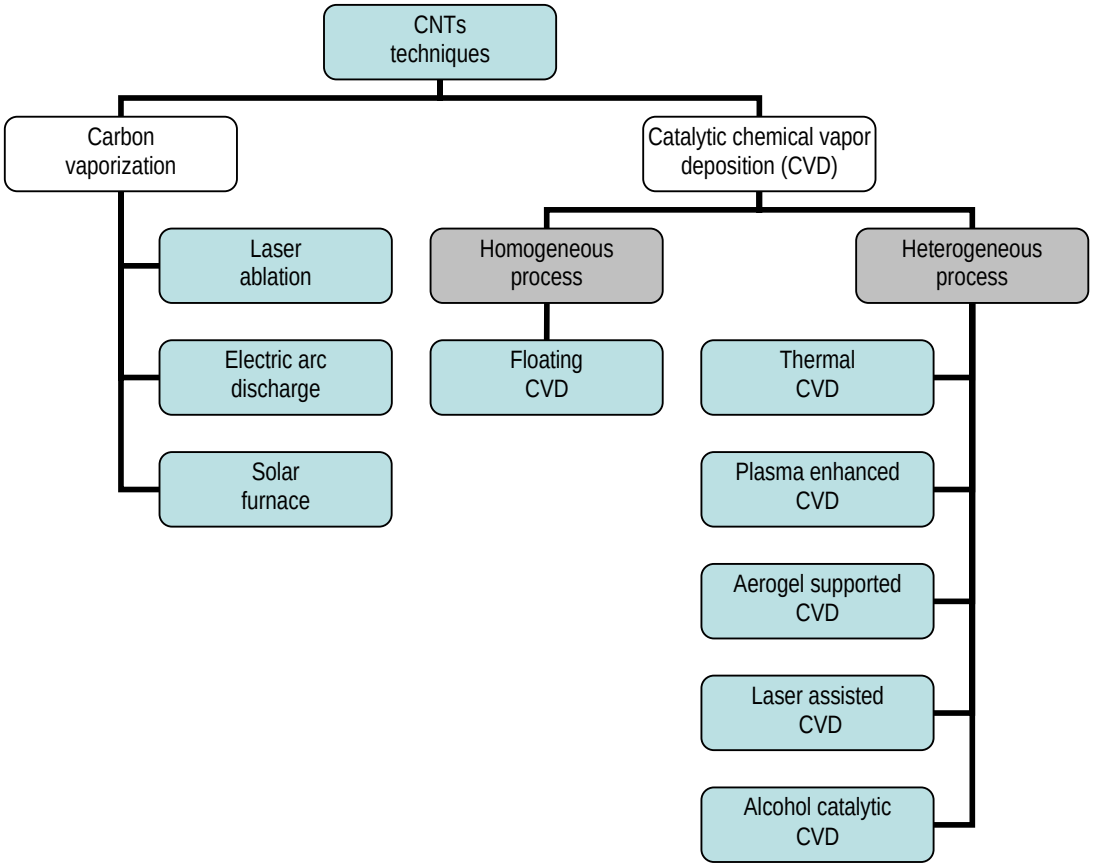

Figure 2.6 Classification of CVD techniques

Just like CNTs, GNFs can be prepared by using electric arc discharge, floating CVD and catalytic CVD (Li et al., 2007). The following section described the respective techniques in detail.

2.6 Carbon vaporization method

The common characteristic of the carbon vaporization method is to prepare CNTs through vaporizing pure carbon or carbon-rich raw materials such as artificial and natural graphite or different types of coals. The reaction is done with or without transition metal catalysts at very high temperature that is between 1000 and 6000 K and different atmospheres. The techniques include electric arc discharge, laser ablation and solar energy vaporization. They are based on one essential mechanism that is the interaction between either the target material and external radiation (laser beam or radiation emanating from solar energy) or the electrode and the plasma (in case of electric arc). This leading to the formation of a plasma, i.e. an electrically neutral ionized gas, composed of neutral atoms, charged particles (molecules and ionized species), and electrons (Bhushan, 2004).

2.6.1 Electric arc discharge

Electric arc discharge was initially used to produce C_{60} fullerences before the first CNTs were discovered using this method. In principle, the method creates nanotubes through arc-vaporisation of two carbon rods separated by approximately 1 mm in an enclosure filled with inert gas such as helium, argon or even nitrogen at low pressure. Then, a direct current of 50 to 100 A is driven by approximately 20 kV creates a high temperature discharge between the two electrodes. As a result, the discharge vaporises one of the carbon rods and forms a small rod shaped deposit on the other rod. The yield of nanotubes depends on the uniformity of the plasma arc and the temperature of the deposit form on the carbon electrode (Daenen et al., 2003). There are two kinds of synthesis can be formed in this arc that are

evaporation of pure graphite and co-evaporation of graphite and a metal (Journet et al., 1998).

2.6.2 Laser ablation

The first achievement of the large-scale synthesis of SWNTs was realized using this method in 1996, where SWNTs with a mean diameter of 1.38 nm were produced (Cheng et al., 2004). In principle, the carbon is vaporized from the surface of a solid disk of graphite into a high-density helium (or argon) flow, using a focused pulsed laser. Initially, a graphite target is placed in the middle of a long quartz tube mounted in a temperature-controlled furnace (refer to Figure 2.7). Once the sealed tube has been evacuated, the furnace temperature is increased to 1200°C. Then, the tube is filled with a flowing inert gas. Later, a scanning laser beam is focused onto the graphite target by way of a circular lens. To maintain a smooth, uniform face for vaporization, the laser beam scans across the target surface. As a result, the laser vaporization produces carbon species, which are swept by the flowing gas from high-temperature zone and deposited on a conical water-cooled copper collector.

Laser's ablation is almost similar to arc discharge, since the optimum background gas and catalyst mix is the same as in the arc discharge process and it can produce two kinds of products. The first one is when just a pure graphite target is used in which MWNTs are found in 4 to 24 graphitic layers. The second product consists of SWNTs when a small amount of transition metal has been added to the carbon target.

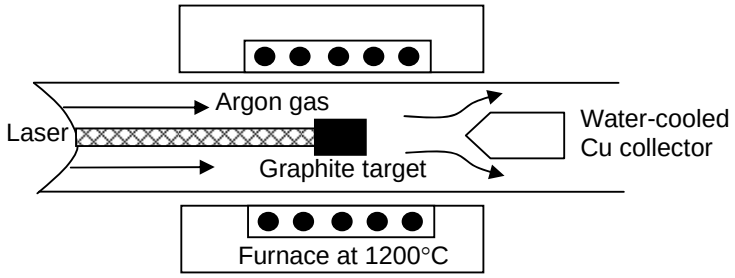

Figure 2.7 Laser ablation (Daenen et al., 2003)

The yield of SWNTs is increasing with temperature. However, the laser evaporation technique yields carbon nanotubes 70% more than that of the electric arc discharge (Journet et al., 1998).

2.6.3 Solar furnace

By using highly concentrated sunlight, solar furnace was first utilized to produce fullerenes but later was modified to produce CNT using more powerful ovens. At the solar furnace, the sunlight is collected by a flat tracking mirror and is reflected towards a parabolic mirror. This mirror focuses the solar radiation directly on the graphite target placed at the center of an experimental chamber (Journet et al., 1998). The principle of this technique is based on the sublimation in an inert gas of a mixture of graphite powder and catalysts formerly placed in a crucible (refer to Figure 2.8).

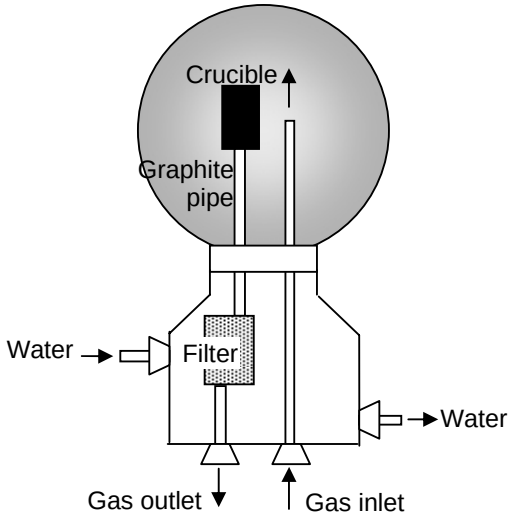

Figure 2.8 Solar experimental chamber (Bhushan, 2004)

2.7 Catalytic chemical vapor deposition

In catalytic chemical vapor deposition (CVD) a catalyst such as iron (Fe), cobalt (Co) and nickel (Ni) have to be applied to synthesize various kinds of CNTs such as

SWNTs, MWNTs, and aligned MWNT arrays (Journet et al., 1998). The catalyst enhanced thermal cracking of gaseous carbon source is commonly referred to as catalytic chemical vapor deposition (CVD). It involves the catalytic decomposition of a carbon containing source that is hydrocarbon or carbon monoxide (CO) on small metallic particles or clusters. The reaction can be achieved either by heterogeneous process (where solid substrate has a role) or homogeneous process (where everything takes place in gas phase) (Bhushan, 2004).

2.7.1 Heterogeneous process

This process basically consists of furnace with catalysts which are transition metal particles (e.g. Fe, Co, Ni) deposited onto a substrate or support (Figure 2.9). The furnace is heated to the desired temperature before passing a gaseous flow containing a given proportion of hydrocarbon gas (e.g. CH_4, C_2H_2, C_2H_4 or C_6H_6 mixed with either H_2 or an inert gas like Ar over the catalyst. The reaction is chemically defined as catalysis-enhanced thermal cracking $C_xH_y \rightarrow xC + y/2H_2$ (Baker, 1978).. Alternatively, CO can be used instead of hydrocarbons, the reaction is the chemically defined as catalysis-enhanced disproportionation $2CO \rightarrow C + CO_2$.

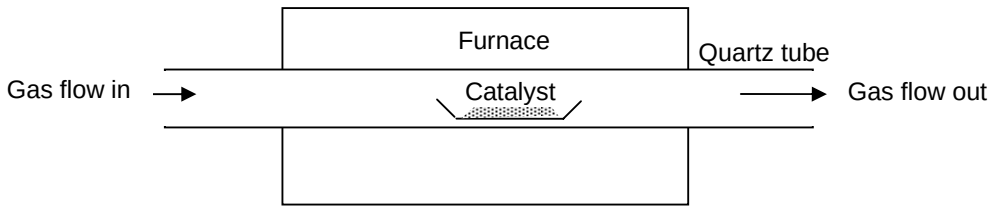

Figure 2.9 Experimental set up used for CCVD (Journet et al., 1998)

There are four structural carbons that could be formed: amorphous carbon layers, filaments of amorphous carbon, graphite layers covering metal particles and MWNTs. Several factors could influence the parameters, for example variation in the size of active metal particle would result in variation of the nanotube diameters. In addition, the length of the developed tube depends on the reaction time. By varying the support and the catalyst, various results can be obtained such as if the

support is graphite and the catalyst is Co, most of the filaments produced are graphitic (Journet et al., 1998). Of all catalysts, it has been reported that Nickel (Ni) offers a better yield as compared with other transition metals (Bououdina et al., 2005; Journet et al., 1997; Shaijumon et al., 2005). However one report claims that Fe-Mo/MgO catalyst can produced a high yield of CNT over 550% relative to the weight of Fe-Mo metal in the Fe-Mo/MgO catalyst (Lyu, Liu, Lee, Park, Kang, Yang, & Lee, 2004a).

2.7.2 Homogeneous process

The homogeneous route also called as floating catalyst method, differs from heterogeneous method because it uses only gaseous species and does not require the presence of any solid phase in the reactor. It is also known as double stage furnace. The first stage is where the metal-organic compound decomposes to generate nanometric metallic particles that can catalyze the nanotubes formation. The second stage is where the carbon source is decomposed to atomic carbon, which is then responsible for the formation of nanotubes.

The typical reactor used in this technique is a quartz tube placed in an oven to which the gaseous feedstock, containing the metal precursor, the carbon source, some hydrogen and a vector gas (N_2, Ar, or He) is sent. The first zone of reactor is kept at a lower temperature, and the second zone, where the formation of the tube occurs is heated to 700-1200°C. The metal precursor is generally a metal-organic compound, such as a zero-valent carbonyl compound like iron pentacarbonyl ($Fe(CO)_5$), or a metallocene e.g. ferrocene, nickelocene or cobaltocene (Bhushan, 2004).

Parameters that are needed to be controlled are the choice of carbon source; the reaction temperature; the residence time; the composition of the incoming gaseous feedstock with a particular attention paid to the role played by hydrogen proportion, which can control the orientation graphenes with respect to the nanotube axis thus switching from c-MWNT to h-MWNT; and the ratio of the metallorganic precursor

to the carbon source (Bhushan, 2004). As for the carbon source, saturated carbon gases tend to produce highly graphitized filaments with fewer walls compare with unsaturated gases. For example, methane and CO commonly used for SWNT while acetylene, ethylene and benzene, which are unsaturated and thus give high carbon are typically used for MWNT (Teo et al., 2003).

2.8 The advantages and disadvantages of catalytic CVD

There are different techniques of CVD depending on the types of reaction, heating sources, carbon source and different deposition space and position of CNTs (Daenen et al., 2003; Journet et al., 1998). Some of the CVD techniques are thermal, plasma enhanced, alcohol catalytic, floating aero gel-supported and laser assisted. Each technique has its own advantages and disadvantages. For example in catalytic CVD (CCVD), the advantages are CNTs can be produced at moderate temperatures as well as low cost and their structures can be tailored by the selection of a given metal (Rodriguez et al., 1995). For both heterogenous and homogeneous processes, CNTs prepared by catalytic CVD are generally much longer (few tens to hundreds of micrometers) than those obtained by arc discharge (few micrometers). However, MWNTs from CCVD contain more structural defects than MWNTs from arc-discharge, due to lower reaction temperature, which does not allow any structural rearrangements (Bhushan, 2004).

The drawback CCVD is that the difficulty to control the size of the metal nanoparticles, and thus the nanotube formation is often accompanied by the production of undesired carbon forms (amorphous carbon or polyaromatic carbon phases found as various phases or as coatings). In particular, encapsulated forms have been often found, as a result of the creation of metallic particles that are too big to be active for growing nanotubes (but are still effective for catalytically decomposing the carbon source) and are totally recovered by graphene layers (Bhushan, 2004). Apart from the two types of processes mentioned, there are other CCVD methods such as *in-situ* catalysis, micropore template and fluid bed methods

as well as different heating sources such as plasma injection vapor deposition and plasma-enhanced chemical vapor deposition have been applied (Cheng et al., 2004).

2.9 Comparison of the three main techniques

Among all the techniques or methods mentioned above, CVD, laser ablation and electric arc discharge are the most popular methods to produce CNT. Table 2.1 gives the comparison among these three techniques where each has its own advantages and disadvantages.

Table 2.1 Comparison among CVD, laser ablation and arc discharge (Daenen et al., 2003; Eklund, 2006)

Description	CVD	Laser ablation	Arc discharge
Process	Batch	Batch	Batch
Purity	High	High	Low
Temperature	Low	High	High
Yield	High (20-100%)	Low (up to 70%)	High (30-90%)
Cost	Low	High	High
SWNT tubes length	Long 0.6-4 nm	Long (5-20 μm)	Short (0.6-1.4 nm)
SWNT wall defects	More	Less	Less
MWNT tube length	Long	*Not reported*	Short (1-3 nm)
Pros	Easy to produce SWNT, few structural defects, cheap	Good diameter, few defects, product is quite pure	Simple process, easy to scale up, diameter controllable, quite pure
Cons	CNTs usually MWNT with deffects	Expensive due to laser and high power requirement	Tubes short and in random sizes, needs purification

2.10 Mechanism of growth in CVD

The growth mechanisms of CNTs and GNFs in CVD are slightly different due to the formation of graphite plane structures.

2.10.1 Growth of CNTs

The growth mechanism of CNT initially begins when adsorption and decomposition of carbon molecules (from carbon source) occur on the surface of the nanoparticles catalyst. Essentially it is assumed that the catalyst particles are spherical (or pear-shaped) and the deposition takes place on only one half of the surface (Daenen et al., 2003). At specific temperature, the catalytic decomposition takes place at the surface of the metal particles. This is followed by a mass-transport of the carbon either by surface or volume diffusion. When the carbon concentration reaches the solubility limit and the precipitation starts (Bhushan, 2004). The growth of nanotubes begins as soon as a supersaturation leads to carbon precipitation and creates a crystalline tubular form. The tube size is determined based on the size of the metal catalyst particle (Dresselhaus, 2006)

In general, the growth mechanism can be either in base-growth mode or tip growth mode. The former mechanism is also known as extrusion or root growth because it occurs in a catalyst support or on substrate (Figure 2.10 (a)). Initially, the carbon feedstock is supplied from the 'base' where the nanotube interfaces with the anchored metal catalyst. Then, the carbon nanofilament grows away from the substrate or support leaving the catalyst nanoparticle attached to the filament (Bhushan, 2004). The nanotubes lengthen with close-end, while the catalyst particle remains on the support surface.

The tip-growth mechanism occurs when the metal-support interaction is weak since the interaction is highly dependent on the type of support materials and the type of metal precursor being used in preparing the catalyst. By referring to Figure 2.10 (b), as a result the catalyst particle lifted off from the support and carried along at the tube end as the nanotube grows (Dresselhaus, 2006).

Saturated carbon gases like methane and carbon monoxide tend to produce highly graphitized filaments with fewer walls that are SWNTs while unsaturated gases like acetylene, ethylene and benzene are typically used for MWNT. (Teo et al., 2003). In addition, the growth of mechanism in CVD is effective throughout the isothermal zone as long as the carbon feedstock is continuously fed. Hence, the longer the isothermal zone in gaseous carbon excess conditions, the longer the nanotubes (Bhushan, 2004).

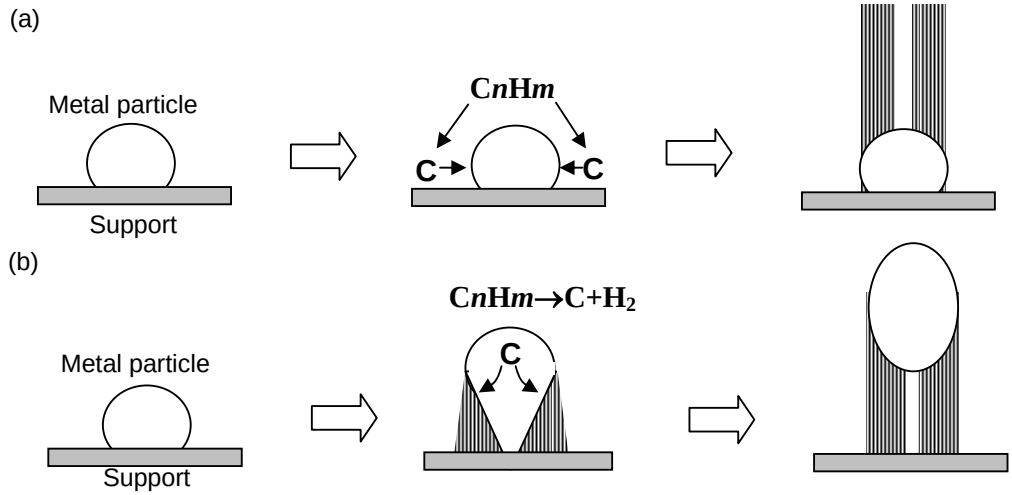

Figure 2.10 (a)Base and (b)tip growth mechanisms of CNTs (Daenen et al., 2003)

As mentioned earlier, formation of MWNT could result in bamboo structures in concentric like *bc*-MWNTs and herringbone like *bh*-MWNTs. This is due to a specificity of the dissolution-rejection mechanism which is periodic, discontinuous dynamics of the phenomenon. During the reaction, once the catalyst has reached the saturation threshold regarding its content in carbon, it expulses it quite suddenly. A little while later it becomes again able to incorporate a given amount of carbon before over-saturation is reached again (Bhushan, 2004). Thus, in bamboo structure, several segments can be seen along the nanotubes.

2.10.2 Growth of GNFs

The mechanism growth of GNF can be referred in Figure 2.11 where①, ② and ③ symbols represent the three steps that are step 1, 2 and 3, respectively in the mechanism process. Initially, step 1 is when the absorption and decomposition of hydrocarbon molecules occur on the surface of metal crystallographic faces (R. T. K. Baker, 2001). At step 2, the dissolution and diffusion of carbon species into the nanoparticles interior occur to form a metal-carbon solid state solution. Next at step 3, nanofibers growth occurs when a supersaturation leads to carbon precipitation into a crystalline tubular form. The size of the metal catalyst nanoparticle generally dictates the diameter of the synthesized nanofiber (Dresselhaus, 2006).

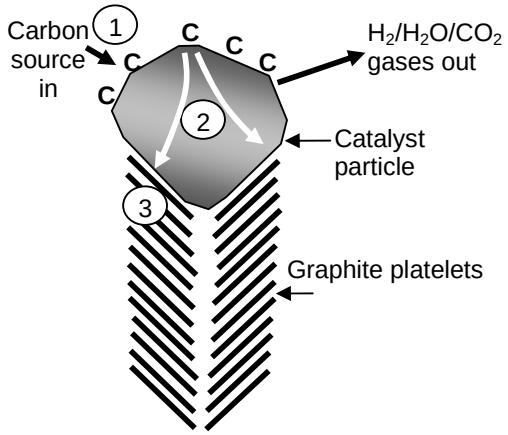

Figure 2.11 Key steps in growth process of graphitic nanofibers

The crystalline perfection degree of the deposited fiber is determined by the catalyst particle chemical nature, the reactant gas composition and the temperature. In Figure 2.12 the graphite platelets are oriented in a "herringbone" arrangement. Surface science studies revealed that only certain faces of metal particle favor precipitation of carbon in the form of graphite. Other faces could deposit less ordered carbon (Baker, 1998). The carbon structure continues to grow as long as the heat balance is maintained in the reaction system. Any perturbations in the chemistry of the leading face of the metal catalyst causes a buildup of solid carbon at this

interface. This results in deactivation and termination in nanofiber growth (Baker, 2001).

Typically, nanostructures are formed by a bidirectional mode where precipitation of carbon occurs simultaneously from opposite faces of the catalyst particle. Hence the catalyst particle remains within the structure throughout the growth process. Conversely, for herringbone case, the carbon deposition process occurs at the sides of the particle that is carried at the tip of the growing fibre. For graphite platelets, the graphene planes are stacked in a direction parallel to the base of the particle and perpendicular to the fibre or filament axis. As for herringbone structure, the particles adopt a rhombic morphology where the nanofibers are precipitated from a pair of opposite faces to generate a structure that is aligned at an angle to the fiber axis (Rodriguez et al., 1995).

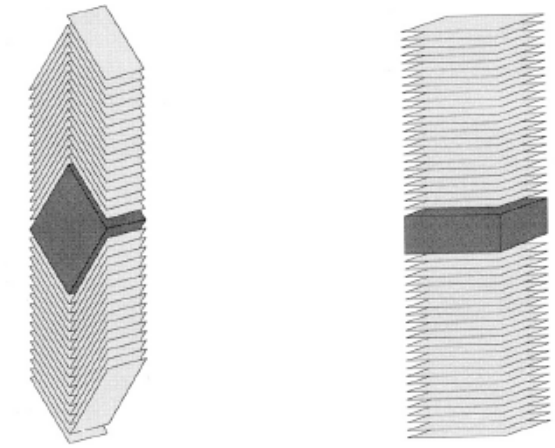

Figure 2.12 GNFs generated from catalyst surface to form (a) platelet and (b) herringbone structures (Rodriguez et al., 1995).

As long as the rate of precipitation of carbon from all four faces is identical, the GNF will be continuously formed as a long straight nanofiber. However, any perturbation in this pattern of behavior will give rise to abnormalities in the conformation of the fibers. As a result, coiled or helical configurations of nanofibers are formed instead (Rodriguez et al., 1995).

2.11 CNT and GNF engineering: Parameters involved

As mentioned in previous section there are several parameters involved in the growth mechanism of both CNT and GNF in the CVD reaction. The parameters are as follow:

2.11.1 Catalyst

Controlling the size of catalyst nanoparticles is crucial since it determines the final diameter of nanotube or nanofiber and the type of nanotube wall (SWNT or MWNT) (Teo et al., 2003) especially in the making of SWNT since only catalyst particle with diameter less than 2 nm is able to produce SWNT filament (Bhushan, 2004). Moreover, particles with diameters smaller than 25 nm will tend to produce nanotubes, whereas larger particles usually generate solid nanofibers.

Apart from metal powder, catalyst can come in different configurations such as gauzes, wires, foils and supported metal particles like alumina and silica (Baker, 2001). The catalysts usually come from transition metal oxides such as Cobalt (Co), Nickel (Ni), Copper (Cu), Molybdenum (Mo), Iron (Fe) as well as their alloys for heterogeneous process and metal-organic compound or a metallocene like ferrocene, nickelocene or cobaltocene for a homogeneous process.

2.11.2 Reactant gases including carbon feedstock

In CVD reaction, there are several types of hydrocarbon gases like ethylene (C_2H_4), acetylene (C_2H_2) and methane (CH_4) as well as carbon monoxide (CO) has been successfully utilized to produce both CNTs and GNFs (Baker, 2001; Bhushan, 2004; Teo et al., 2003). In addition benzene and xylene are used as carbon feedstock, especially in a homogeneous process. Unsaturated gases like C_2H_4, C_2H_2 and benzene are used to synthesize MWNTs since they have a high carbon content, whereas saturated gases like CO and CH_4 are used to synthesize SWNTs since they tend to produce highly graphitized filaments and fewer walls (Teo et al., 2003). Along with these carbon rich gases and vapors, hydrogen is used to reduce the metal

particles (that is oxides) during the heating as well as to decrease the formation of carbon deposits from pyrolysis of the carbon feedstock. Moreover, carrier gas such as argon, helium or nitrogen is used to flush the reactor initially to create an inert atmosphere.

2.11.3 Reaction temperature

The reaction temperature in CVD is much less as compared with electric arc discharge, which can reach up to 4000 K. For CNTs synthesis the operating temperature is between 500 to 1100°C (Journet et al., 1998) while GNFs can be synthesized between 400 to 1000°C (Baker, 2001). The variation of the temperature depends on the catalyst activity, experimental configurations and carbon feedstock. Any temperature higher than 1000°C could result in more formation of amorphous carbon (Teo et al., 2003).

2.11.4 Reaction time

The reaction time varies from minutes to hours depending on the gas flowrates and the length of the reactor. It is thought that prolong the reaction time resulting in longer CNTs and GNFs produced. However, longer reaction hour could result in more carbon deposits. Table 2.2 shows some works on CNTs and GNFs done by researchers. From the table, it can be concluded that CH_4 and CO were used to synthesize SWNT while C_2H_4 and C_2H_2 were used to synthesized MWNTs and GNFs. As for catalyst, majority used Ni for GNFs production and Fe for CNTs production which can be in the form of metals, films, alloys and different types of catalyst supported.

Table 2.2 Summary of the developed carbon nanomaterials

Structure	C-source	Catalyst	Reference
SWNT	CH_4	Al_2O_3-SiO_2 of 5g	(Cassell et al., 1999)
	CO	Fe/Mo 50 mg	(Zheng et al., 2002)
	CH_4	Fe:Mo=6:1	(Hornyak et al., 2002)
	CO	0.1-0.5 g $Fe(CO)_5$	(Huang et al., 2003)
	C_2H_4	1 g Fe-Mo/MgO	(Lyu et al., 2004b)
	nil	Ferrocene	(Barreiro et al., 2006)
MWNT	C_2H_2	Fe, SiO_2 substrate	(Lee et al., 2001)
	toluene	$FeCl_3$	(H. Hou et al., 2003).
	CH_4, CO_2	Ni/MgO	(Branca et al., 2004)
	CH_4	Pd or Ni-Fe	(Shah et al., 2004)
	C_2H_2	silica with iron film	(Yao et al., 2004)
	C_2H_2	$MmNi_2$, $MmFe_2$	(Shaijumon et al., 2005)
	CO	Fe/Al_2O_3 2g	(Li et al., 2005)
	C_2H_2	ferrocene 100 mg	(Shaijumon & Ramaprabhu, 2005)
GNF/ CNF	CO	0.2 g Ni	(Kayiran et al., 2003)
	C_2H_4	98 mg Ni, 2 mg Cu	(Luxembourg et al., 2003)
	CH_4	Co on MgO, Al_2O_3, SiO_2	(Takenaka et al., 2004)
	C_2H_4	Cu:Fe, Cu:Ni	(Lueking et al., 2004)
	C_2H_4	metal powder	(Rzepka et al., 2005)
	CH_4/C_2H_4	Ni/carbon	(Takehira et al., 2005)
	C_2H_4	Ni/Y zeolite based	(de Lucas et al., 2005)
	C_2H_4, CO	Ni-Fe 100 mg	(Yu et al., 2005)
	CH_3CN	$Fe(C_5H_5)_2$	(He et al., 2005)
	C_2H_4	Ni/graphite microfibers	(Pham-Huu et al., 2006)
	C_2H_4	Bimetallic Fe-Cu	(Marella et al., 2006)

2.12 Properties of CNT and GNF

Properties of CNTs depend on whether they are SWNTs or MWNTs. Even properties of SWNTs may also change depending on whether single SWNT or SWNT ropes are being formed. SWNTs are stable up to 750°C in air and up to 1500 to 1800°C in inert atmosphere. Both physical and chemical properties of SWNTs are related to their unique structural features. Properties of MWNTs are not

much different from that of regular polyaromatic solids, which exhibit graphitic, turbostratic, or intermediate crystallographic structure.

The variations are mainly driven by textural type of the MWNTs such as concentric, herringbone, bamboo and the quality of the nanotexture (Bhushan, 2004). The properties of GNFs are almost similar with that of CNTs. Therefore, only few studies have been done to highlight the properties of GNFs especially in comparison to CNTs. The following section describes the properties of CNTs based on research work carried out by other researchers.

2.12.1 Surface area

Theoretical specific surface area of CNTs ranges from 50 to 1315 m^2/g. This broad scale depends on the number of walls, the diameter, or the number of nanotubes in a bundle of SWNTs. Experimentally, the specific surface area of SWNTs is often larger than that of MWNTs. Typically, the total surface area of as-grown SWNTs ranges between 400 and 900 m^2/g with micropore volume between 0.15 and 0.3 cm^3/g. On the other hand, as produced MWNTs have the total surface area between 20 and 400 m^2/g are often reported (Bhushan, 2004).

2.12.2 Electrical conductivity

CNTs can be either semi-conducting or highly conducting (metallic), depending on their chiral vector. Their conductivity has been shown to be a function of their chirality, the degree of twist and their diameter (Nanovip.com, 2006). The differences in conducting properties are due to molecular structure, which results in a different band structure and band gap. These can easily be derived from the graphene sheet properties (Daenen et al., 2003). For example, a nanotube is metallic when $n=m$ and $n-m=3q$ where n and m are the integers that specify the tube's structure and q is an integer. This means that all armchair SWNTs are metallic, one-third of zig-zag and chiral tubes are metallic and the rest is semiconducting (Harris, 1999).

2.12.3 Thermal conductivity and expansion

The temperature stability of CNTs is estimated to be up to 2800°C in vacuum and 750°C in air. It is expected that CNTs are able to transmit up to 6000W/(m·K) at room temperature as compare to copper which can only transmit at 385 W/m·K. Even ultra-small SWNTs have been shown to exhibit superconductivity below 200 K. The strong in-plane graphitic C-C bonds make them exceptionally strong and stiff against axial strains. In addition, the almost zero in-plane thermal expansion but large inter-plane expansion of SWNTs implies strong in-plane coupling and high flexibility (Nanovip.com, 2006).

2.12.4 Chemical reactivity

A chemical reactivity of a CNT is enhanced due to the curvature of the CNT surface. As the curvature increases, the reactivity, which is directly related to the *pi*-orbital mismatch also increases. Hence, a great distinction between the sidewall and the end caps of a nanotube should be distinguished. Depending on solvents used, covalent chemical modification of either sidewalls or end caps is possible. Moreover, a smaller nanotube diameter also results in increased reactivity (Daenen et al., 2003).

2.12.5 Mechanical strength and elasticity

In their axial direction, CNTs have a very large Young modulus since as a whole, the material is very flexible due to the great length. (Daenen et al., 2003). The tube is considered to have lower Young's modulus when it is a solid cylinder. Conversely, when the tube is hollow and the tube's wall gets thinner, the modulus gets higher (Adams, 2000). It is reported that SWNTs are stiffer than steel and have a resistant to physical force damage (Nanovip.com, 2006). CNTs have high bending strength due to their hexagonal network which, can partly transform into pentagons and heptagons to release the exerted stress (Lu et al., 2004).

2.12.6 Optical activity

CNTs show strong structured optical spectra, since they are one-dimensional systems (Reich et al., 2004). Theoretical studies claimed that when the nanotubes become larger, the optical activity of chiral nanotubes disappears. The density of states of the highest occupied energy level that is Fermi Level, are zero for semiconducting and approximately to zero for metallic CNTs (Nanoledge, 2007). Hence, it is expected that other physical properties are influenced by these parameters. Use of the optical activity might result in optical devices in which CNTs play an important role (Daenen et al., 2003)

2.12.7 Field emission

Field emission occurs due to the tunneling of electrons from a metal tip into vacuum, under application of a strong electric field. Because of their small diameter and high aspect ratio, CNTs is very favorable for field emission (Nanovip.com, 2006). Emission has been observed at fields lower than 1 V/μm and high current densities over 1 A/cm^2. MWNTs are identified to be more robust than SWNTs since the latter have multiple shell architecture that provide more stable structure upon ion bombardment and irradiation associated with field emission (Sarrazin, 2005).

2.12.8 High aspect ratio

For maximum stress transfer to occur a fiber must have a certain minimum aspect ratio that can be defined as l_c/d where l_c and d are the critical length and the diameter of a material, respectively (Harris, 1999). As compared to conventional additive materials such as carbon blackor stainless steel fiber, CNTs and GNFs as excellent additives to impart electrical conductivity in plastics. Their high aspect ratio (about 1000:1) imparts electrical conductivity at lower loading (Cheap Tube Inc, 2007).

2.12.9 Adsorbent

Due to the large surface area and high absorbency, CNTs are ideal material for the use in air, gas, and water filtration. Some ongoing researches are trying to replace activated charcoal with CNTs for ultra high purity applications (Nanovip.com, 2006). Besides separation process, apart from GNFs, CNTs are potential to be a storage system for hydrogen gas in onboard vehicles.

2.13 Potential applications

The unique and outstanding physical and chemical properties of GNFs and CNTs have given some exciting opportunities for exploitation of them in several applications. Various applications of GNFs and CNTs can be referred in Table 2.3 and Table 2.4, respectively. It is estimated that the global market for GNF would increase from $48 million in 2007 to $176 million in 2012 and grow to $825 million by 2017.

Table 2.3 Applications of GNFs

Industry	Applications	References
Automotive	Fuel systems, paintable parts, exterior panels	(Grupo Antolin, 2007)
Electronic	Packaging materials for ESD sensitive items, hard disk drive and semiconductor manufacturing, EMI shielding,	
Energy	Bipolar and end plates, electrode catalyst support in PEM fuel cells, hydrogen storage	
Aerospace	High performance conductive adhesive, microelectronics sensors, nanocomposite rocket ablative materials	
Chemistry	Catalyst support	

Table 2.4 Applications of CNTs

Industry	Applications	References
Nano-fabrication	CNT probes for SPM, AFM, sensors, nano-pumps, nano-channels, nano-gears, etc.	(Ajayan et al., 2001; Cheng et al., 2004; Nguyen, 2005; Subramoney, 2001)
Electronic materials/devices	Nano-transistors, nanowires, memory devices, digital logic circuits, single electron tunneling (SET),	(Barrera et al., 2005; Cheng et al., 2004; Yamada, 2005)
Biotechnology	Injection devices, bio-sensors, nano-capsules, FET-based biosensors;	(Cheng et al., 2004; Jun, 2005)
Chemistry	Nano-reactors, chemical sensors, catalyst, catalyst support, thermal sensor, resonator sensors	(Cheng et al., 2004; Jing, 2005)
Composite materials	Reinforcements for polymeric, metallic, ceramic and conductive composites, electromagnetic, etc.	(Ajayan et al., 2001; Barrera et al., 2005; Calvert, 1997; Daenen et al., 2003)
Electrode materials, energy storage	Supercapacitors, battery electrodes, lithium ion batteries	(Ajayan et al., 2001; Calvert, 1997; Daenen et al., 2003)
Electron sources	Field effect transistors (FET), field emitters, flat panel display, cold cathode x-ray tubes, etc.	(Ajayan et al., 2001; Calvert, 1997; Cheng et al., 2004; Sarrazin, 2005; Yamada, 2005)

2.14 Methods of adsorption measurement

For a strong adsorbed solute of limited solubility, an adsorption capacity of an adsorbent for the specific solute is defined as the value of the amount of adsorbed substance reached in a saturated solution (IUPAC, 1997). To achieve the adsorption capacity, gas adsorption equilibria can be measured using different methods like

volumetry or manometry, gravimetry, densietry, oscillometry, calorimetry and chromatography (Keller et al., 2005). Among these methods, for hydrogen physical adsorption measurement, volumetric and gravimetric measurements are often used.

Volumetric or manometric measurement is based on the measurement of the gas pressure in a calibrated constant volume at a given temperature (Thommes, 2004). The working principle of this conservative method is simple. Initially a given amount of adsorbate gas is expanded in a vessel filled with adsorbent which is previously evacuated. During the expansion, part of the gas adsorbed on the internal and external surface of the adsorbent while the remaining part as the gas phase around the adsorbent. If the void volume of the adsorbent is known, by mass balance equation, the amount of gas, which has been adsorbed can be calculated (Keller et al., 2005).

The first gravimetric adsorption measuring instruments were believed to be hygrometers in 1450 (Kiefer et al., 2008). However, the idea of using gravimetric measurement began at the end of nineteenth century when there was a lack of highly sensitive balances able to measure small relative changes in the weight of a sorbent sample e.g 10^{-6} g/g or even less. In 1912 Emich described an electronic beam microbalance to investigate adsorption and a coil spring balance. Later, a design of electro-magnetically compensated two beam microbalance was used in 1965 by Sartorius, Göttingen in Germany before a single beam magnetic suspension balance (MSB) was developed by Lösch, Kleinrahm and Wagner in 1980s (Keller et al., 2005). This measurement is achieved by mounting a sample (adsorbent) in a microbalance. Next sample activation by evacuation, heating and flushing with Helium is done before the sample is evacuated in order to measure the mass of the sample. Later the sorptive gas is introduced which leads to change in the balance's record due to gas adsorbed onto the surface adsorbent and buoyancy effects of the sample in the surrounding gas. Both volumetric and gravimetric give significant contributions in adsorption measurement as well as some drawbacks as indicated in Table 2.5 (Keller et al., 2005). From the table, it can be seen that gravimetric measurement has lots of advantages as compared with volumetric measurement. Nevertheless, majority of the literatures reported the use of volumetric

measurements in hydrogen adsorption instead of gravimetric measurement as stated in Table 2.6.

Table 2.5 The advantages and disadvantages of volumetric and gravimetric measurements (Keller et al., 2005).

Volumetric	Gravimetric
Advantages: • The precision in measuring techniques is accurate. • Simple and does not require sophisticated equipment. **Disadvantages:** • Certain amount of sorbent is required to note considerable changes in the gas pressure due to adsorption. • Thermodynamic equilibrium of adsorption is unsure. • Pure sorptive gas could adsorbed onto walls of adsorption vessel and tube connection. • The uncertainties of the adsorbed mass accumulated due to algebraic structure of the sorptive gas mass balance equation. • The change of sorbent mass due to activation and degassing can only be taken into account after the experiment. • No information on the process kinetic • Not useful in extreme low and high pressure due to inaccuracy in Equation of State (EOS).	**Advantages:** • High reproducibility, sensitivity and accuracy up to 10^{-8} of measurements. • Need only little amount of sorbent • Thermodynamic equilibrium of adsorption can be determined. • Information on kinetics of adsorption process is known. • No problem in pure gases adsorb on walls of tubes and vessels. • No problem in extreme low and high pressure measurement. • The change of sorbent mass due to activation and degassing can be taken into account during the measurement. **Disadvantages:** • Sensitive to electromagnetic and mechanical disturbances. • Equipment is expensive, sophisticated and complex. • Measurements are laborious i.e. need to run buoyancy and blank tests prior to adsorption measurements. • Fine grained sorbent or powders might be blown out due to sorptive gas flow.

Table 2.6 Summary of hydrogen storage capacity using carbon as adsorbent

	Adsorbent	Conditions	Uptake (wt%)	Reference
Volumetric	SWNT	107.9 kPa, 77 K	2.37	(Nishimiya et al., 2002)
	GNF	170 bar, 77 K	0.22	(Kayiran et al., 2003)
	SWNT	60 bar, 253 K	1	(Luxembourg et al., 2003)
	MWNT	135 bar, 293 K	4.6	(Hou et al., 2003)
	MWNT	120 bar, 77 K	2.27	(Ning et al., 2004)
	MWNT	80 bar, 298 K	2.4	(Shaijumon & Ramaprabhu, 2005)
	SWNT	100 bar, 298 K	1.8	(Lachawiec et al., 2005)
	AC	70 bar, 77 K	4.5	(Panella et al., 2005)
	CNF	100 bar, 303 K	0.35	(Blackman et al., 2006)
	Pd doped CNF	90 bar, 298 K	0.59	(Back et al., 2006)
	Pd loaded Maxsorb	90 bar, 298 K	0.7	(Ansón et al., 2006)
	Activated carbon	100 bar, 298 K	0.85	(Jin et al., 2007)
Gravimetric	Activated carbon	125 bar, 298 K	1.5	(Ströbel et al., 1999)
	graphite nanocrystals	70 bar, 298 K	0.8	(Badzian et al., 2001)
	GNF	20 bar, 300 K	0.29	(Lueking et al., 2005)
	GNF	140 bar, 298 K	0.4	(Rzepka et al., 2005)
	carbide derived carbon	1 atm, 77 K	3	(Gogotsi et al., 2005)
	GNF	80 bar, 298 K	0.18	(Hong et al., 2006)
	Activated carbon	1 atm, 77 K	2.7	(Figueroa-Torres et al., 2007)
	Ni plated CNF	100 bar, 298 K	2.2	(Kim et al., 2008)

It presents the result of H_2 adsorption using a different type of carbon materials including activated carbon, CNT and GNF. The conditions vary with temperature between 77 K to room temperature and pressure between atmospheric pressure to148 bar. The results of H_2 uptake vary from 0.11 to 6.3 wt% depending on the pressure and temperature conditions as well as types of material used as an adsorbent. The highest uptake recorded by (Hou et al., 2003) with H_2 uptake of 6.3 wt% with purified MWNT as adsorbent using volumetric measurement at 148 bar and 298 K. Regardless of what type of measurement that a researcher decides to take up in hydrogen adsorption experiment, careful procedures need to be taken into consideration since amount of hydrogen adsorbed on carbon materials is much smaller than that of other gases like methane. These include apparatus leakage,

temperature control, time for equilibration of pressure, gas purity and amount of sample used as the adsorbent (Takagi et al., 2004).

Based on the literature reviews conducted, limited studies have been carried out in measuring H_2 adsorption onto CNTs and GNFs by gravimetric measurement technique that is using magnetic suspension balance or MSB. Most of the hydrogen adsorptions were done by volumetric measurement and few of them use gravimetric measurement. Only Hong et al. used MSB but up to pressure 80 bar. Others used intelligent gravimetric analyzer or IGA (Lueking et al., 2005) and modified Sartorius Supermicro S3D-P (Rzepka et al., 2005; Ströbel et al., 1999). Moreover, majority of the samples used have been modified or treated such as purification, carbonization and exfoliation (Hong et al., 2006; Lueking et al., 2005; Poirier et al., 2001). Such treatments are costly if the materials are put into commercialization and at most of the times does not improve the uptake (Viswanathan et al., 2003) In addition, hydrogen adsorbed in purified and pretreated material could not be completely desorbed at room temperature. Moreover, part of the pore structure could permanently destroyed by hydrogen storage (Hou et al., 2003).

As for GNF and CNT, although the synthesis have been done using catalysts such as ferrocene (Barreiro et al., 2006; He et al., 2005; Shaijumon & Ramaprabhu, 2005; Singh et al., 2002), iron (Edwards et al., 2006; Hornyak et al., 2002; Hou et al., 2003; Lee et al., 2001; Li et al., 2005; Lueking et al., 2004; Lyu et al., 2004a; Zheng et al., 2002) and nickel (Bououdina et al., 2005; Branca et al., 2004; Che et al., 1998; Kayiran et al., 2003; Luxembourg et al., 2003; Shah et al., 2004; Ting et al., 2006; Yu et al., 2005), but none of them have used Taguchi method as part of their design of experiment in order to optimized the reaction yield. In addition, for simulation and theory of hydrogen adsorption isotherm modeling, a study of predicting isotherm using assumption free model has yet been developed.

Thus, this research would close the gaps that exist by:

1. Synthesizing GNFs as well as CNTs and applying Taguchi method for the design of experiment.
2. Using as-synthesized GNFs for H_2 adsorption and desorption studies.

3. Using gravimetric measurement that is IGA at 77 K and pressure up to 20 bar as well as MSB at room temperature and pressure up to 150 bar.
4. Predicting hydrogen isotherm for various surface area of adsorbent using Neuro-fuzzy system.

2.15 Summary

Carbon nanomaterials are among the most potential materials to store H_2 in onboard vehicle. Although many researchers have begun their study in hydrogen adsorption using these materials, but particular attention on GNF study should be explored more as it has a potential to store hydrogen as the interlayer spacing between the graphene layers is sufficient enough to accommodate hydrogen molecules only but not other bigger gas molecules. Furthermore, unlike activated carbon, GNF could retain the hydrogen molecules at room temperature (Baker, 1998) and can be desorbed easily as compared with CNT. Thus, an investigation on hydrogen adsorption onto GNF using gravimetric measurement at high pressure is crucial to fulfill part of hydrogen economy's aspirations. Gravimetric measurement is chosen since it has significant advantages over volumetric measurement such as less amount of sample is needed to put on test for adsorption, high reproducibility, sensitivity and accuracy of measurement, as well as problems in extremely low and high pressure measurement are preventable.